

# Tomography Systems and Sensor Application for Sharp-Edged Delta Wing Analysis

Mohamed Salman Sikandar Bathusha<sup>1</sup>, Shabudin Mat<sup>1\*</sup>, Fahmi Izzuddin<sup>1</sup> and Khushairi Amri Kasim<sup>1</sup>

<sup>1</sup>School of Mechanical Engineering, Universiti Teknologi Malaysia, 81310 UTM Skudai, Johor, Malaysia.

\*Corresponding author: shabudin@utm.my, Tel: 607-5534614

**Abstract:** This paper presents the results on wind tunnel testing above non-slender sharp-edged delta wing under pitching motion. Above the sharp-edged delta wing the flow topology is very complex, disorganized and unresolved till date. The primary vortex onset is occurred at the wing apex of the sharp leading-edge delta wing and it develops from the leading edge of the wing to the trailing edge. There are several factors that influenced the vortex properties above the wing such as angle of attack, Reynolds number, Mach number, leading-edge bluntness and flow control techniques. The main objective of this study is to show the flow control technique effects known as the blower, above the sharp-edged non-slender delta wing on the flow topology. The experiments were carried out in the wind tunnel at Reynolds number of  $0.8 \times 10^6$  with the speed of 25m/s. A generic delta wing model was fabricated in UTM with a sweep angle of  $55^\circ$ , the model was designed to be installed to UTM Aerolab external strain gauge. During the experiments, the blowers were placed at three different positions 15%, 50% and 70% from the Apex of the wing and these locations are named as *location I, II and III*. In order to measure the vortex, a measurement technique called as surface pressure measurement was employed on the wing. The experiments were divided into two phases. The first phase was the clean wing configuration where the experiment was performed without the flow control. The final experiment was the experiments with the flow control at three different locations. The results have shown that the location of blower has influenced the flow characteristics above the wing. The result obtained shows that the blower at location I has an impact at higher angle of attack while with the blower at location II and III, the blower has significantly increased the primary vortex in size and at the high angle of attack the vortex breakdown is considerably delayed.

**Keywords:** Sharp-edged delta wing, Vortex Flow Experiment (VFE), Active Flow Control, Primary Vortex, Wind Tunnel Experiment.

© 2021 Penerbit UTM Press. All rights reserved

*Article History: received 25 May 2021; accepted 12 June 2021; published 15 October 2021*

## 1. INTRODUCTION

The theoretical and experimental study of sharp-edge delta wing aerodynamic characteristic has been the subject of interest in supersonic aircraft for many years, both subsonic and supersonic speed ranges. The Reynolds number, leading-edge bluntness and angle of attack determines the primary vortex of the leading-edge. Primary vortex formation towards the aft portion of the delta wing can be delayed by the increase in leading-edge bluntness and Reynolds number (Shabudin Mat et al, 2017).

The vortex origin is fixed from the apex of sharp leading-edge delta while pitching motion for a certain angle of attack, where the primary vortex onset is situated in the wing apex. There are some factors such as Mach number, Reynolds number and angle of attack which affects the formation of the primary vortex. As the primary vortex approaches the trailing edge the magnitude of the primary vortex suction peak decreases (Luckring, 2014).

For the sharp-edged delta wing the secondary vortex is also generated in counter rotating direction of the primary vortex in which the adverse pressure gradient is developed in the direction of the flow. For the sharp-edged delta wing the secondary vortex is formed nearer to the apex region

(Rodriguez, 2008). The vortex origin, primary vortex, secondary vortex, inner vortex and the vortex breakdown for the sharp-edged delta wing is investigated under both pitching angles with and without active control to study the aerodynamics flow above the delta wing.

## 2. LITERATURE REVIEW

At an angle of attack, a strong shear layer formed along the leading edge of the sharp-edged delta wing flow topology, causes flow separation. The primary vortex is created by spiral fashion motion of the strong shear layer, as the primary vortex travel downstream the intensity increases. Because of the strong side flow towards the leading edge a secondary vortex is formed underneath the primary vortex as the angle of attack increases. (Luckring, 2014).

Coton et al (2008) showed that above the delta wing with sharp-edge, the angle of attack has an impact on the flow topology. The onset of the flow separation travels upstream towards the apex of the wing if the angle of attack is raised, and at a high angle of attack the secondary separation line is specifically shown. The sharp leading vortex shape is not impacted by the Reynolds number. This declaration is proven by the Hummel, 2004. His experiment on pressure distribution on the sharp-edged

delta wing reveals that there is no effect on vortex formation at high and low numbers of Reynolds. This is because the primary separation in the sharp-edged case is set at the apex.

### 2.1 Non-Slender Delta Wing Flow Field

Dual vortex structure is visible in the flow of a non-slender delta wing. The interaction between the primary shear layer and the secondary vortex, according to Gursul *et al.* (2005), produces a dual vortex structure. The primary vortex is divided in two when the secondary vortex comes into contact with it. The dual vortex structure mechanism has also been explained by Brett & Ooi (2014). The outcome of Brett & Ooi's (2014) CFD on the 45° sweep delta wing shows the primary vortex, shear layer separation and double vortex or shadow vortex.

There are vortical currents and vortex breakdowns often at low attack angles, such as a few degrees. The curious aspect was the incidence at angle of attack 2-5° breakdown over the wing. One would not usually expect to experience a breakdown at such a low incidence, particularly as far forward on the wing. At low incidences, the surface flow patterns also clearly show the existence of primary reattachment and secondary separation lines, implying the existence of strong vortical flows over the lifting surface. The reattached line shifts inboard towards the wing's centerline as the incidence of the wing increases. For an angle of attack of 15 degrees, the secondary line of separation exhibits a curvature shift at roughly 30 to 40% of the apex chord length. This is more likely to be the outcome of vortex breakdown than the boundary layer transition on this non-slender wing (Gursul 2004).

### 2.2 Effects of Angle of Attack on Non-Slender Delta Wing

The characteristics of the vortex breakdown are also determined by the attack angle. The angle of attack upstream influences the rate of vortex breakdown. At a greater angle of attack, the twin vortex system does not develop. This is owing to the outboard vortex on the wing's weaker structure at a higher angle of attack. The vortex breakdown occurs earlier at 2.5° degree angle of attack (Taylor *et al.* 2003).

### 2.3 Active Flow Control Over Delta Wing

Active flow control is a technique for controlling the vortical flow above delta wings that has several advantages, including increasing or delaying flow separation, enhancing lift force, reduction of drag, reducing wing and fin buffeting, and suppressing or enhancing turbulence. Vortex strength, location, and structure are modified using active and passive flow control techniques. Furthermore, active flow control techniques have a significant impact on performing various objectives throughout various flight routines, and these flow control techniques manipulate the following flow topology: shear layer detachment, vortex development, flow separation and reattachment, and vortex breakdown control (Gursul *et al.*, 2007). In the F2 subsonic, closed-return, and atmospheric wind tunnel at ONERA's Fauga-Mauzac Center, Renac *et al.* tested a

narrow delta wing with a sweep angle of 60 degrees. To provide continuous jet mass normal to the leading edge and parallel to the leeward side of the wing, four hole locations on the leading edge were chosen. The results revealed that a stable and powerful vortex formed in the vicinity of the blowing hole. The development of a vortex on the left side of the wing where a continuous mass jet was used, but no vortex on the right side where no blowing technique was used (Renac *et al.*, 2005).

Delaying the vortex breakdown and shifting its location towards the trailing edge is enhanced by increasing the blowing mass flow rate. This occurs as a result of the trailing edge's strong adverse pressure gradient being handled. Figure 8 shows the location of the vortex core and the vortex breakdown, with the position of the vortex breakdown shifting downstream.

The purpose of this research is to determine the impacts of blower-type active flow control on a non-slender delta wing with a sharp edge at different locations and angles of attack. The initial location will be at the apex of the wing, which is comparable to Mitchell *et al.* (2001)'s core blowing. The second and third positions are at 50% and 70% of the model's apex, respectively. The outcome will be expressed as in the form of aerodynamic coefficient.

## 3. METHODOLOGY

The model in Figure 1 has a strong leading edge in this project. The purpose of developing this model is to examine the impact of different blower configurations and flow topologies above the delta wing on different angle of attack. At Reynolds number  $0.8 \times 10^6$  at equal wind speeds of 25 m/s, the tests were carried out at the angle of attack varying from  $\alpha = 0^\circ$  to  $\alpha = 18^\circ$ . Reynolds number is calculated using Mean Aerodynamic Chord (MAC) of 0.4937m.

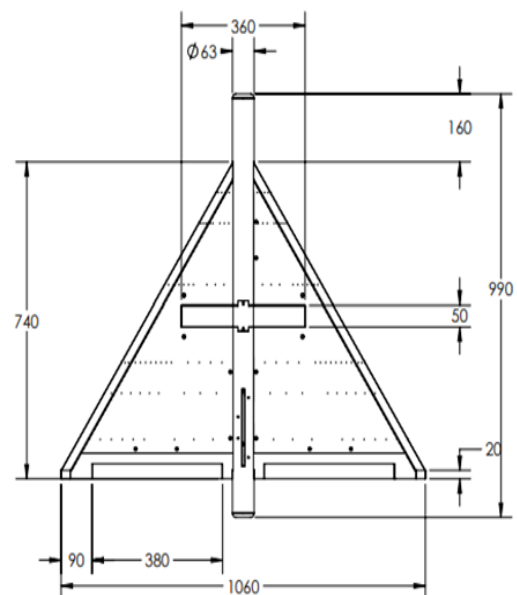


Figure 1. The geometry of UTM delta wing model

The experiment was conducted in a Low Speed Wind Tunnel (UTM-LST) at Universiti Teknologi Malaysia with dimensions of 2.0m (width), 1.5m (height), and 5.8m (length) which has a maximum speed of 80 m/s. For this research, six holes were drilled in the leading edge of the wing. The experiments were carried out at a speed of 25 m/s, which corresponded to  $0.8 \times 10^6$  Reynolds numbers, with various angles of attack ranging from  $0^\circ$  to  $18^\circ$  in  $3^\circ$  increments. The delta wing's dimensions are listed in Table 1.

Table 1. Dimensions of delta wing model

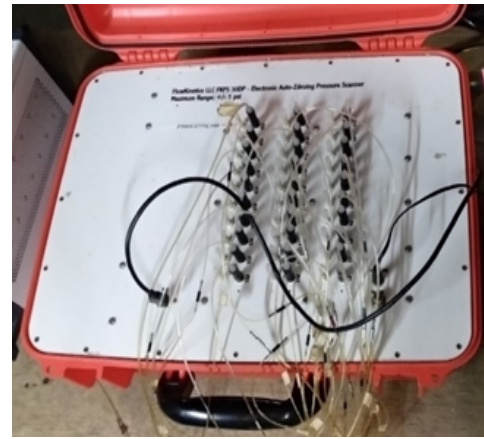
Part	Dimension
Fuselage length (core)	990 mm
Sweep angle	$55^\circ$
wingspan (max)	1061 mm
wing chord (max)	743 mm
Mean aerodynamic chord	493.8 mm
Diameter of fuselage	66 mm
Height	216 mm

For the analysis, only 3 holes are needed, while the other 3 are for model stability during testing. The position of the holes are 15 percent of the apex of the core (location I or 148.5 mm from the apex), 30 percent of the apex of the core (location II or 297 mm from the apex) and 70 percent of the apex of the core (location III or 693mm from apex).

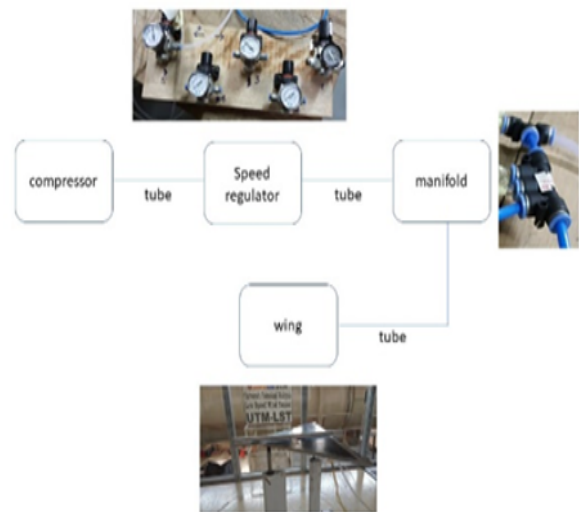
The blower holes distribution around the surface of delta wing shown in figure 2 measured using a pressure tubes to be installed inside the delta wing with the assist of pressure scanner shows in Figure 3. The data recorded in the Lab Via application at the wind tunnel facility. A compressor was used to blow up the model's surface. From the compressor to the speed regulator, six sets of tubes were mounted. The speed controller is used to control the blow rate. The blowing rate is 35m/s for this experiment. The flow will go through manifolds from the speed regulator. The arrangement of the blowing distribution is shown in the Figure 3.



Figure 2. Blower positions along the leading edge



(a)



(b)

Figure 3. (a) Pressure Scanner and the (b) Distribution of the flow by the blower located in the delta wing

## 4. RESULTS AND DISCUSSION

The surface pressure measurement result from the experiment is discussed in this section. The actual surface pressure data from the wind tunnel test had been transformed into pressure coefficients ( $C_p$ ). The clean wing and the configuration with the blower at position I, II & III are studied.

### 4.1 Pressure Coefficient of the clean with all blower configuration

In this section, the effect of adding an active flow control (blower) at three distinct points on the flow topology is investigated.  $y/c_r$  was 0.05 in the first position, 0.3 in the second, and 0.7 in the third. The results of the blower experiment are compared to those of a clean wing design. The results of blowing on the data on surface pressure are discussed in this section.

The angles  $3^\circ$  and  $6^\circ$  are the chosen angles for the low angle of attack area. In Figure 4, the combination graph of all positions at  $\alpha = 3^\circ$  is shown. It is found from the figure that there are no improvements in  $C_p$ . This resulted because the delta wing was unable to provide the required

lift at low angles and low flight speeds (Kwak and Nelson, 2010).

The application of blowing at position I at  $\alpha = 6^\circ$  allows the  $C_p$  to decrease about 10 percent, 20 percent, 65 percent and 90 percent at  $y/cr$  as seen in Figure 5. Woods and Roberts (1987) clarified this phenomenon, noting that the vortex has not completely formed at a low angle of attack, so the blowing application would interrupt and degrade the vortical flow and the  $C_p$ .

The angles  $9^\circ$  and  $12^\circ$  are the chosen angles for the medium angle of attack area. In Figure 6, the combination graph of all positions at  $\alpha = 9^\circ$  is shown. The attached flow detaches regularly from the trailing edge and shifts

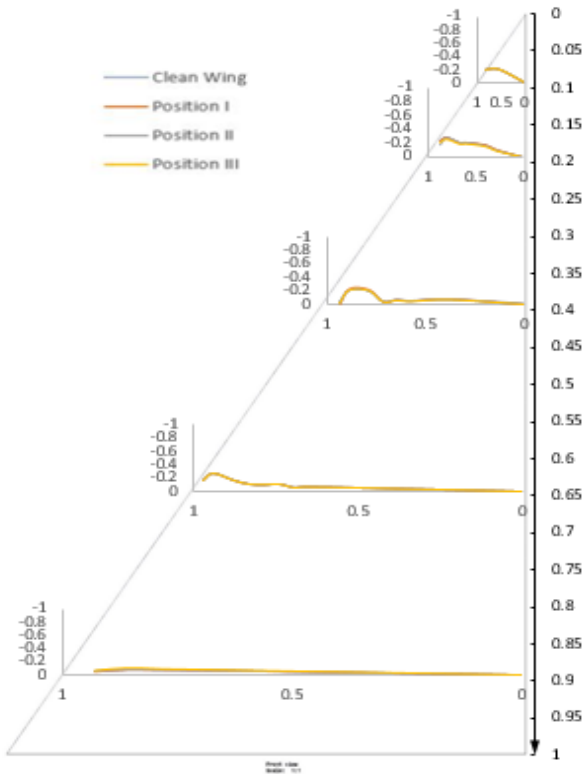


Figure 4. Cp graph for all configuration at  $\alpha = 3^\circ$

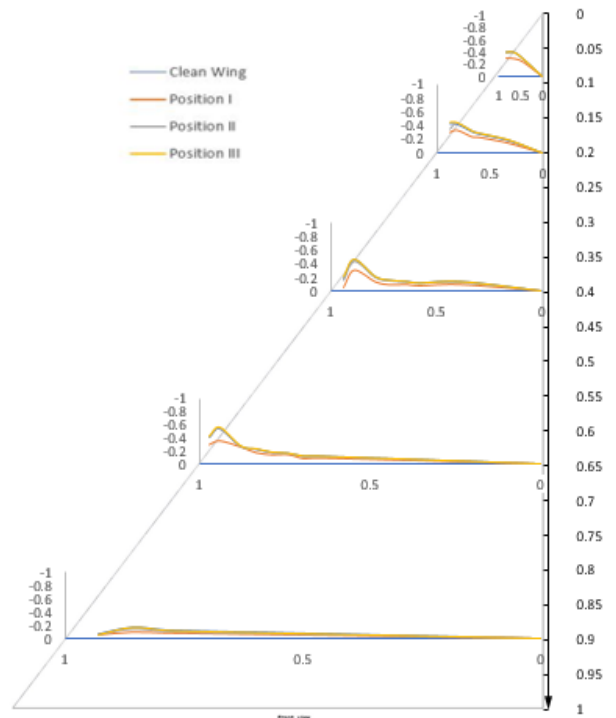


Figure 5. Cp graph for all configuration at  $\alpha = 6^\circ$

to the leading edge, where the suction peak is centered. The major vortex forms at  $y/cr = 40\%$  at  $12^\circ$ , which is sooner than the  $9^\circ$  that arises at  $y/cr = 65\%$ . The result of blowing, however, is not evident at all angles, except at position II.

The combination of all the configuration at  $\alpha = 12^\circ$  is shown in the Figure 7, the vortex shifts inboard toward the centre for the blowing at Position II shows the vortex has shifted inboard at  $y/cr = 40\%$  and  $60\%$ .

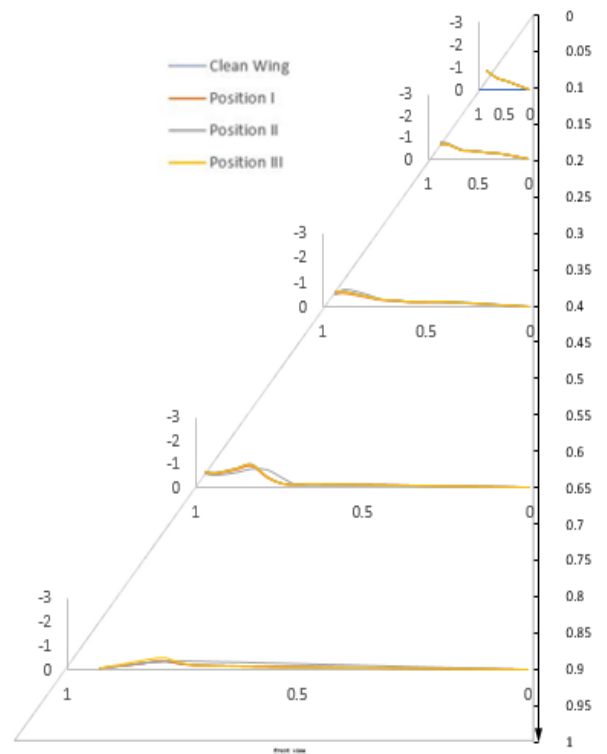


Figure 6. Cp graph for all configuration at  $\alpha = 9^\circ$

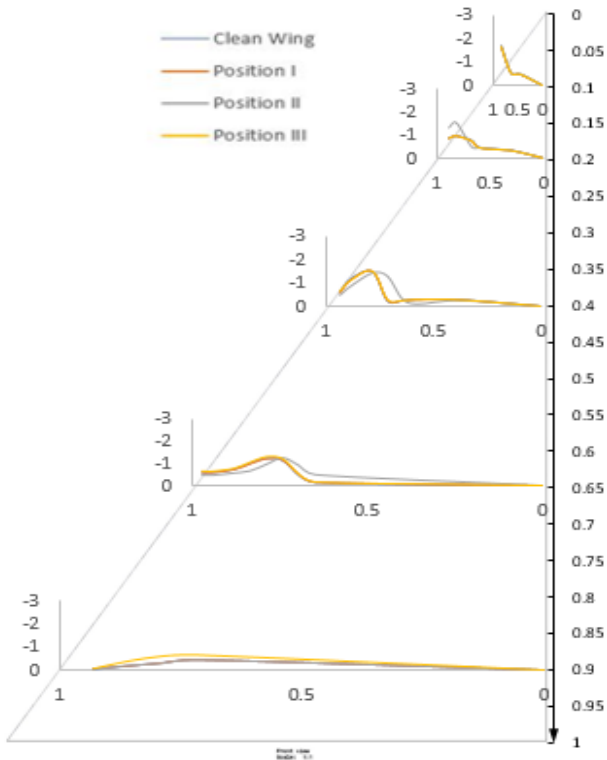


Figure 7. Cp graph for all configuration at  $\alpha = 12^\circ$

At increasing angles of attack ( $15^\circ$  and  $18^\circ$ ), the size of the primary vortex increases at the leading edge. The flow has separated from the wing, resulting in a significant increase in the suction peak. At location II, the effect of blowing can still be seen at  $15^\circ$  and  $18^\circ$  angles of attack.

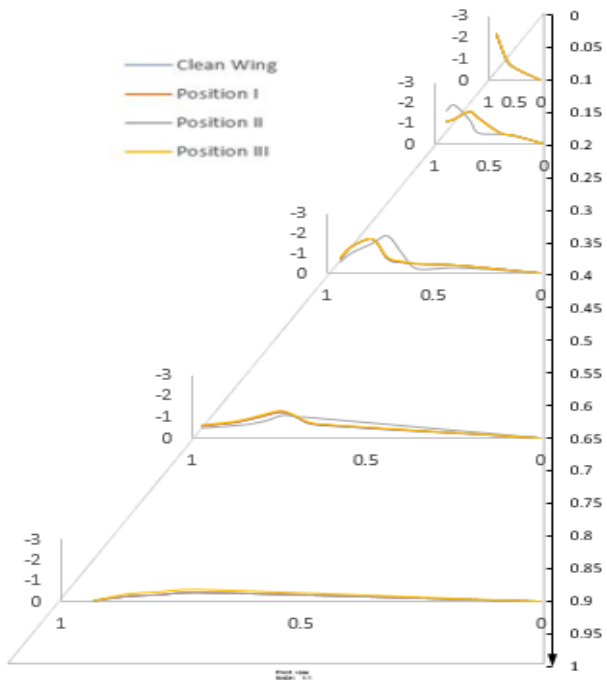


Figure 8. Cp graph for all configuration at  $\alpha = 15^\circ$

#### 4.2 Contour pressure plot

The Contour pressure plot at  $\alpha = 0^\circ$  in all configurations is shown in the figures 10, 11, 12 and 13. The surface pressure contours obtained from the tests were analyzed using the Kriging method. However, in order to attain a better resolution topology, this method

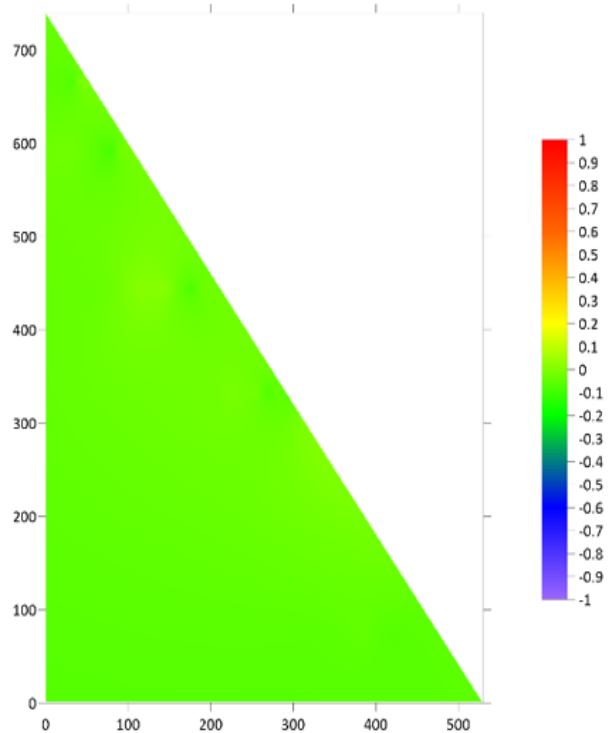


Figure 10. Contour Pressure plot for no blower configuration at  $\alpha = 0^\circ$

For both angle of attack  $15^\circ$  (Figure 8) and  $18^\circ$  (Figure 9), blowing exhibit position II raises the pressure coefficient at  $y/cr = 20$  percent, 40 percent and 65 percent. Positions I and III indicate no changes in the pressure coefficient at both angles.

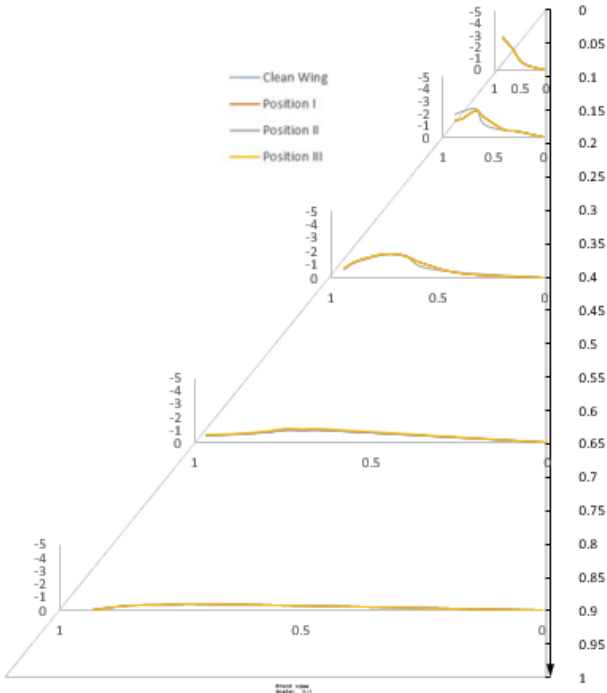


Figure 9. Cp graph for all configuration at  $\alpha = 18^\circ$

need a large amount of pressure data with a uniform distribution. The key constraint in this analysis was the limited number of pressure taps which is only 50. The clean wing's surface pressure topology is compared to the other three blower positions. The small number of pressure taps (50) was a major hindrance in our research.

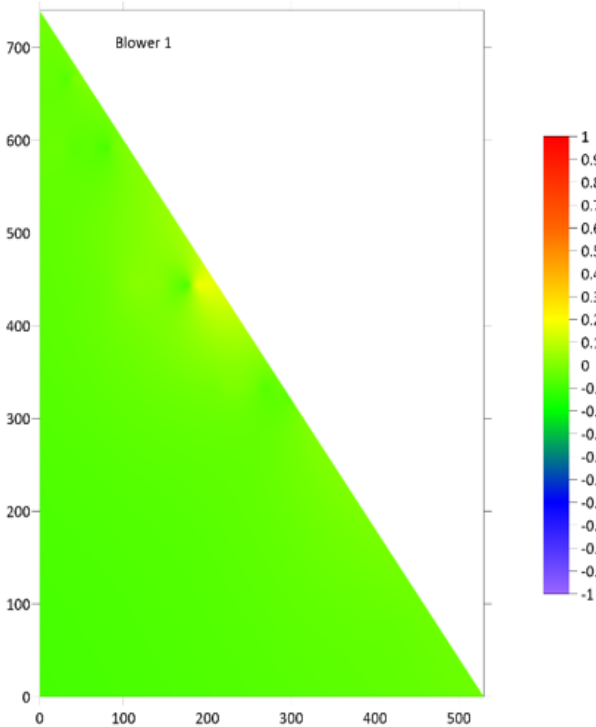


Figure 11. Contour Pressure plot for blower 1 configuration at  $\alpha = 0^\circ$

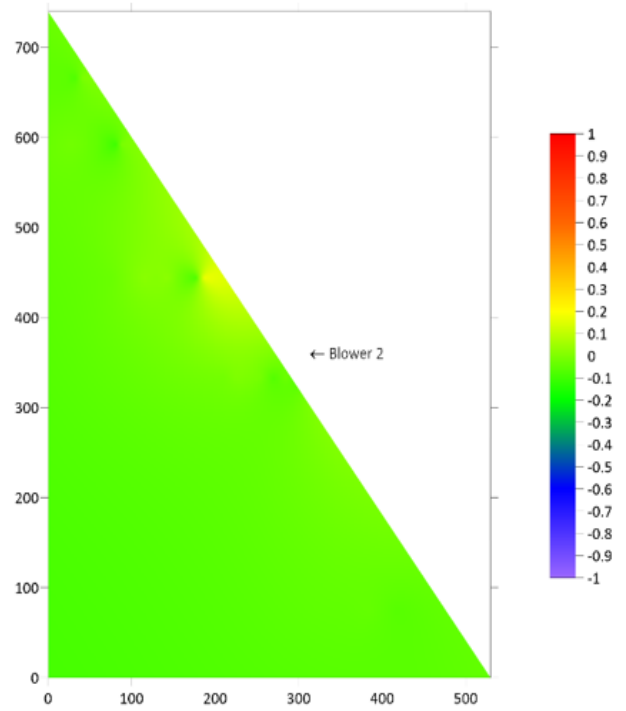


Figure 12. Contour Pressure plot for blower 2 configuration at  $\alpha = 0^\circ$

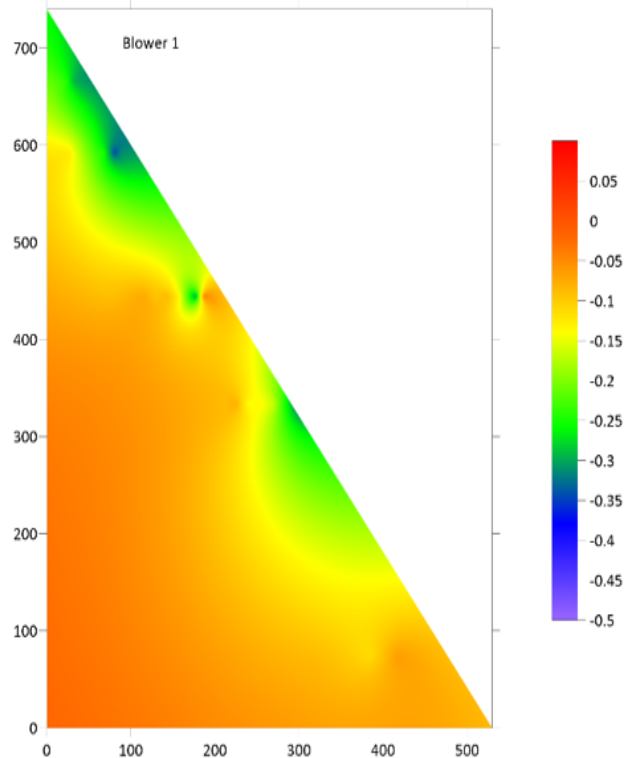


Figure 14. Contour Pressure plot for blower 1 configuration at  $\alpha = 6^\circ$

As seen in Figure 14, blowing at position I at  $\alpha = 6^\circ$  reduces the vortex size across the delta wing's leading edge. Woods and Roberts (1987) clarified this phenomenon, noting that the vortex has not completely formed at a low angle of attack, so the blowing application would interrupt and degrade the vortical flow. The

attached flow detaches from the trailing edge and shifts to the leading edge, where the suction peak is

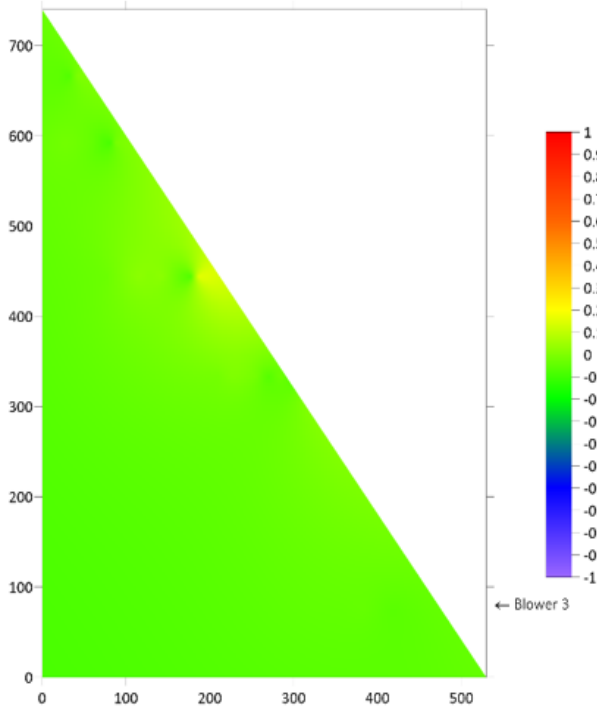


Figure 13. Contour Pressure plot for blower 3 configuration at  $\alpha = 0^\circ$

leading edge of the delta wing at both angle of attack  $9^\circ$  and  $12^\circ$ , as seen in Figures 15 and 16. The result of blowing, however, is not evident at all angles, except at position II.

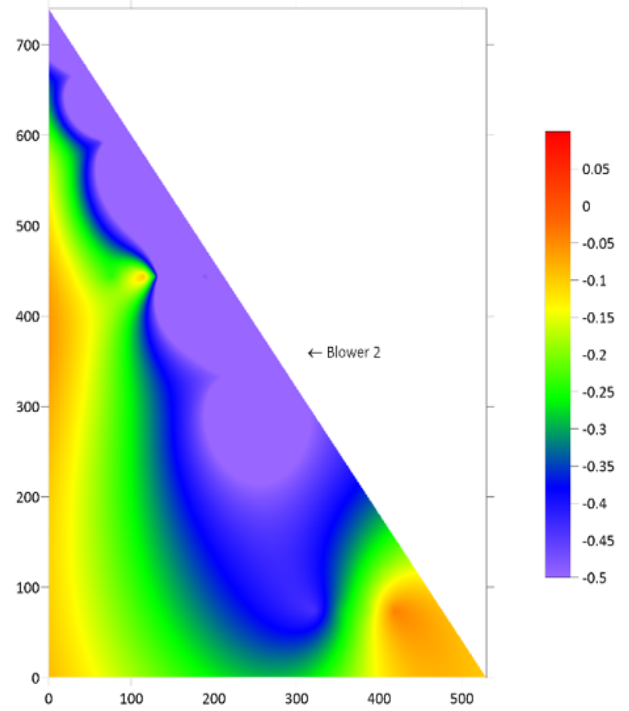


Figure 16. Contour Pressure plot for blower 2 configuration at  $\alpha = 12^\circ$

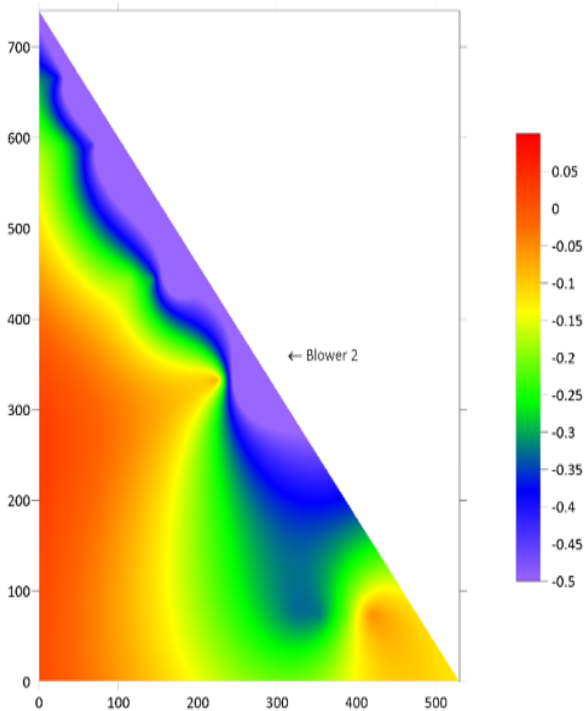


Figure 15. Contour Pressure plot for blower 2 configuration at  $\alpha = 9^\circ$

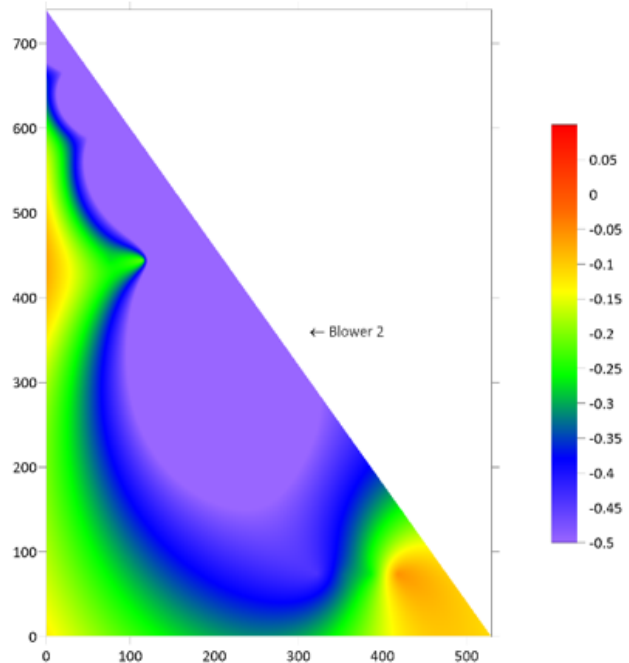


Figure 18. Contour Pressure plot for blower 2 configuration at  $\alpha = 15^\circ$

concentrated. The major vortex emerges 40 percent of the delta wing from the apex at  $12^\circ$ , as opposed to 65 percent of the delta wing from the apex at  $9^\circ$ . At the blower II configuration, the vortex size is enhanced along the

Applying a blow to the rear portion just affects the flow in the rear area. In Figure 17, blowing at location III reveals improvements in the form of a rise in vortex magnitude 90 percent for  $\alpha = 12^\circ$  explains the blower has significant effect on the size of surrounding vortex.

At increasing angles of attack ( $15^\circ$  and  $18^\circ$ ), the size of the primary vortex increases at the leading edge. At location II, the impact of blowing can still be seen at  $15^\circ$  and  $18^\circ$  angles of attack. The vortex size is extended for the blower II configuration at the position 50 percent of the delta wing for both angle of attack  $15^\circ$  (Figure 18)

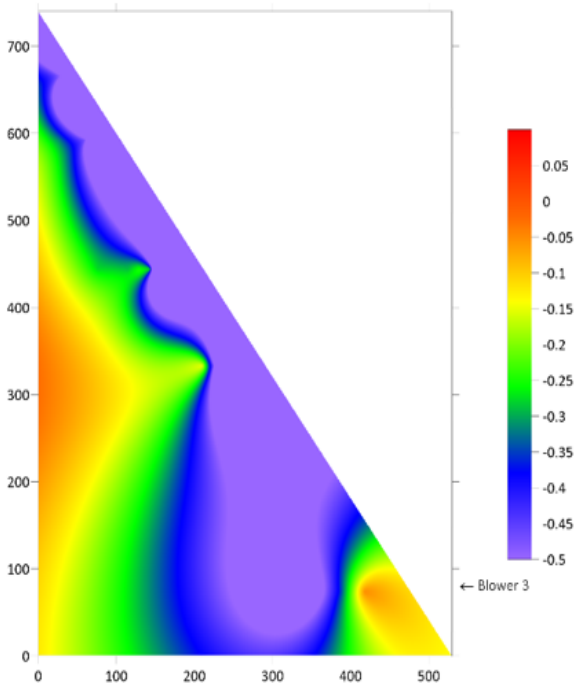


Figure 17. Contour Pressure plot for blower 3 configuration at  $\alpha = 12^\circ$

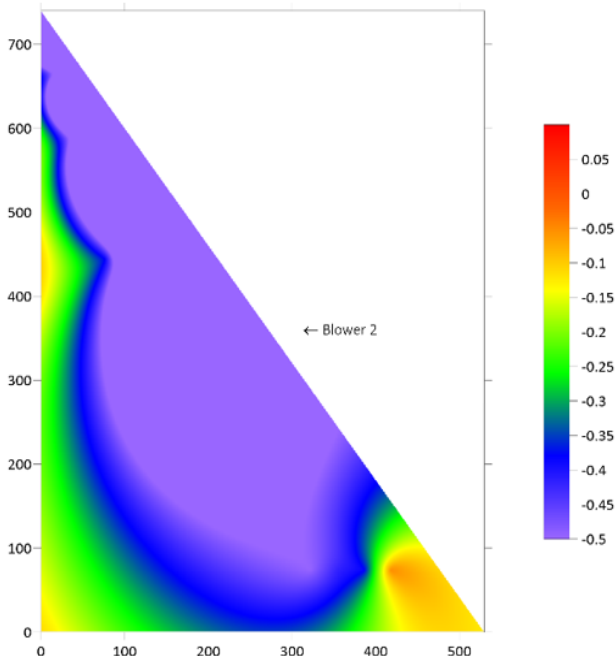


Figure 19. Contour Pressure plot for blower 2 configuration at  $\alpha = 18^\circ$

and  $18^\circ$  (Figure 19), indicating that the blower has a substantial influence on the size of the surrounding vortex. Positions I and III indicate no changes in the pressure

coefficient at both angles.

The primary vortex's size and trajectory have been modified by the installation of Blower at various positions. This study indicates that using a blower can considerably delay the vortex breakdown process (Kasim et al, 2020).

## 5. CONCLUSION

The flow on a non-slender delta wing with sharp edges is complex, with a complicated vortex structure. The purpose of this research was to investigate the impact of different blowing locations on vortex characteristics on the surface of a non-slender delta wing model with sharp edges. A surface pressure measuring methodology was used in the wind tunnel experiment. The contour pressure figure, which was mentioned previously, shows the impacts of blowing configuration on flow topology of the sharp edged non-slender delta wing.

From the research it was also noticed that the blowing effects of the blower can increase the size of the primary vortex. The flow control technique can also improve the aerodynamic properties, according to this study's findings.

The surface pressure data indicates that the blowing arrangement has influenced the vortex characteristics on the wing surface. Blowing had such an impact on the vortex because it changed the flow behavior on the wing based on the locations. At position I, the blowing disrupted the flow at a low angle of attack, but at a higher angle of attack, the blowing effect is negligible.

The vortex breakdown occurs before the delta wing's angle of attack reaches its maximum. The vortex size decreases across the leading edge of the delta wing at low angle of attack, as seen by the contour pressure map. For angle of attack more than 9 degrees, the vortex size is extended for the blower position III arrangement in the aft of the delta wing, indicating that the blower has a substantial influence on the size of the surrounding vortex. At high angles of attack, the blower has a substantial influence on the size of the vortex formation, delaying the vortex breakdown.

## ACKNOWLEDGMENT

This research was funded by the grants from MOHE and Universiti Teknologi Malaysia (21H05 & 4F 832). The experiments have been carried out in Universiti Teknologi Malaysia Aerolab.

## REFERENCES

- [1] Brett, J., & Ooi, A., "Effect of Sweep Angle on the Vortical Flow Over Delta Wings at an Angle of Attack of  $10^\circ$ ," *Journal of Engineering Science and Technology*, 9(6), 768-781, 2014.
- [2] Coton, F. N, Mat, S, Roderick, A.McD, Galbraith & Gilmour, R., "Low Speed Wind Tunnel Characterization of the VFE-2 Wing," *American Institute of Aeronautics and Astronautics*, 2008.
- [3] Gordnier, R. E., & Visbal, M. R., "Higher-Order Compact Difference Scheme Applied to the Simulation of a Low Sweep Delta Wing Flow," 41st Aerospace Sciences Meeting and Exhibit (pp. 1-15). Reno: *AIAA*, 2003.



- [4] Gursul, I., "Recent developments in delta wing aerodynamics," *The Aeronautical Journal*, 108(1087), 437–452, 2004.
- [5] Gursul, Ismet & Wang, Zhijin & Vardaki, Eleni., "Review of Flow Control Mechanisms of Leading-Edge Vortices," *Progress in Aerospace Sciences*. 43. 246-270. 10.1016/j.paerosci.2007.08.001, 2007.
- [6] Hummel, D. J., "Effects of Boundary Layer Formation on the Vortical Flow Above Slender Delta Wings," *Enhancement of NATO Military Flight Vehicle Performance by Management of Interacting Boundary Layer Transition and Separation*. RTO-MP-AVT-111, 2004.
- [7] Luckring, J. M., "Chapter 4- Experimental Investigation of the Flow about A 65° Delta Wing in the NASA Langley National Transonic Facility," *NASA Langley Research Center*; Hampton, VA, United States, 2014.
- [8] Mat, S., Abdullah, M. F., Dahalan, MD. N., Said, M., Abdul-Latif, A., Mansor, S & Lazim, T. M. (2017). Effects of Synthetic Jet Actuator (SJA) on Flow Topology of Blunt-edged UTM VFE-2 Wing Model. AIAA SciTech Forum, 55th AIAA Aerospace Sciences Meeting Grapevine, Texas.
- [9] Mitchell, A., Morton, S., Molton, P., & Guy, Y., "Flow Control of Vortical Structures and Vortex Breakdown Over Slender Delta Wing," *Advanced Flow Management: Part A – Vortex Flows and High Angle of Attack for Military Vehicles*. Loen: RTO AVT, 2001.
- [10] Renac, F, Barberis, D & Molton, P., "Control of Vortical Flow over a Rounded Leading-Edge Delta Wing," *American Institute of Aeronautics and Astronautics*, 2005.
- [11] Taylor, G. S., Schnorbus, T., & Gursul, I., "An investigation of vortex flows over low sweep delta wings," 33rd AIAA Fluid Dynamics Conference and Exhibit (pp. 1-13). Orlando: *AIAA*, 2003.
- [12] Kasim, K. A., Mat, S., Ishak, I. S., & Mansor, S., "Propeller locations study of a generic delta wing UAV model," *Aircraft Engineering and Aerospace Technology*, 2020.